2.4 Intrabeam Scattering

Michel Martini, Fanouria Antoniou, Yannis Papaphilippou
CERN, 1211 Geneva 23, Switzerland
Mail to: Michel.Martini@cern.ch

2.4.1 Introduction

Intrabeam scattering (IBS) consists in the diffusion effects caused by multiple Coulomb scattering on charged particle beams in a storage ring, in both the transverse and the longitudinal beam dimensions. This phenomenon induces the growth in beam emittances and, in some situations, leads to the redistribution of partial beam emittances and energy spread. Thereby, it can cause undesirable beam dilution in phase space or could heat the beam as a whole, i.e. increase the partial beam emittances and energy spread simultaneously. Different comportment results from scattering depending on whether the ring operates below or above transition.

Below transition, small-angle scattering between particles is analogous to particle collisions in a gas, where collisions lead to an equilibrium beam distribution. Above transition, the longitudinal behaviour differs from the one below transition; namely, an energy rise entails a longitudinal velocity decrease as the revolution frequency decreases. The analogy with particles in a gas is no longer valid. Instead, above transition, both the transverse emittances and (longitudinal) energy spread can all grow indefinitely, the energy for the growing oscillation amplitudes being supplied by the radio frequency system.

In the following, we review the conventional IBS Piwinski and Bjorken-Mtingwa formalisms for bunched beams covered in Refs. [1-2], with adaptation of the original Piwinski theory [1] to include the variations of the optical parameters [2], [3]. The Zenkevich Monte Carlo IBS simulation formalism Refs. [11-12] based on binary collision models are also discussed in Refs. [14-15]. Finally, the benchmarking of the IBS theoretical models with Monte-Carlo codes is being presented before the conclusion.

2.4.2 Piwinski Model

2.4.2.1 *Collisional Momentum Kinematic and Emittance Variations*

According to Piwinski [1], for two particles, labelled 1 and 2, colliding with each other, the momentum changes in longitudinal and transverse directions for particle 1 can be written as follows, with $\delta\vec{p}_1 = \delta p_{s_1}\hat{s} + \delta p_{x_1}\hat{x} + \delta p_{z_1}\hat{z}$:

$$\frac{\delta\vec{p}_1}{p} = \frac{\vec{p}_1' - \vec{p}_1}{p} = \begin{cases} \frac{1}{2}\left[2\gamma\alpha\cos\bar{\phi}\sin\bar{\psi} + \gamma\xi(\cos\bar{\psi} - 1)\right] \\ \frac{1}{2}\left[\left(\zeta\sqrt{1 + \frac{\xi^2}{4\alpha^2}}\sin\bar{\phi} - \frac{\xi\theta}{2\alpha}\cos\bar{\phi}\right)\sin\bar{\psi} + \theta(\cos\bar{\psi} - 1)\right], \\ \frac{1}{2}\left[\left(\theta\sqrt{1 + \frac{\xi^2}{4\alpha^2}}\sin\bar{\phi} - \frac{\xi\zeta}{2\alpha}\cos\bar{\phi}\right)\sin\bar{\psi} + \zeta(\cos\bar{\psi} - 1)\right] \end{cases} \quad (1)$$

where $p = |\vec{p}|$ is the mean particle momentum, $\bar{\psi}, \bar{\phi}$ are the scattering and azimuthal angles in the centre of mass (CM) of a two particles collisional event and γ is the Lorenz factor.

The variable ξ, θ, ζ will be used as integration variables for the averaging process of the particle density distribution inside a bunch, γ is the Lorenz factor:

$$\xi = \frac{p_1 - p_2}{\gamma p}, \quad \theta = \frac{p_{x_1} - p_{x_2}}{p} \equiv x_1' - x_2', \quad \zeta = \frac{p_{z_1} - p_{z_2}}{p} \equiv z_1' - z_2', \tag{2}$$

$$2\alpha = \alpha_1 + \alpha_2 = \sqrt{(x_1' - x_2')^2 + (z_1' - z_2')^2} = \sqrt{\theta^2 + \zeta^2}. \tag{3}$$

A particle velocity in the CM frame is assumed non-relativistic i.e. $\bar{\beta} = \sqrt{1 - \bar{\gamma}^{-2}} \ll 1$ and the particle angles made with the longitudinal axis are small, $\xi, \theta, \zeta \ll 1$.

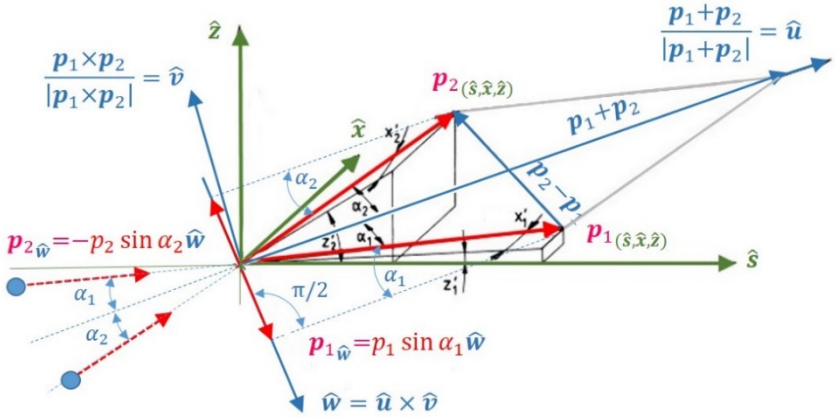

Figure 1: Connexion between the LAB coordinate system $(\hat{s}, \hat{x}, \hat{z})$ and the overlaid $(\hat{u}, v, \hat{w})$ coordinate system aligned on the CM motion (cf. Piwinski [1]).

The invariants of the motion are the transverse emittances $\varepsilon_{x,z}$ (Courant–Snyder invariant) and the quantity H for the longitudinal plane assuming a bunched beam.

$$\varepsilon_x = \gamma_x x_\beta^2 + 2\alpha_x x_\beta x_\beta' + \beta_x x_\beta'^2, \quad H = \left(\frac{\Delta p}{p}\right)^2 + \frac{1}{\Omega_s{}^2}\left[\frac{d}{dt}\left(\frac{\Delta p}{p}\right)^2\right]^2, \tag{4}$$

where $\alpha_x, \beta_x, \gamma_x$ are the Twiss parameters, with $\beta_x\, \gamma_x - \alpha_x^2 = 1$, $2\alpha_x = -\beta_x'$ and Ω_s is the synchrotron frequency.

The alteration in the particle momenta after collision leads to a corresponding change in the particle invariants. Supposing the transverse particle locations stay fixed over the collision time allows calculating the invariant change. The change $\delta\varepsilon_{x,z}$ and δH in the invariant after a single scattering event can be written as:

$$\begin{aligned} \delta H &= 2\frac{\Delta p}{p}\frac{\delta p}{p} + \left(\frac{\delta p}{p}\right)^2, \\ \frac{\delta\varepsilon_x}{\beta_x} &= -\frac{2}{\beta_x}\left[x_\beta(\gamma_x D_x + \alpha_x D_x') + x_\beta' \widetilde{D}_x'\right]\frac{\delta p}{p} + \frac{D_x^2 + \widetilde{D}_x^2}{\beta_x^2}\left(\frac{\delta p}{p}\right)^2, \\ &\quad + 2\left(x_\beta' + \frac{\alpha_x}{\beta_x}x_\beta\right)\frac{\delta p_x}{p} + \left(\frac{\delta p_x}{p}\right)^2 - \frac{2\widetilde{D}_x}{\beta_x}\frac{\delta p}{p}\frac{\delta p_x}{p}, \end{aligned} \tag{5}$$

where $D_{x,z}$ are the horizontal and vertical dispersions, $\widetilde{D}_{x,z} = \alpha_{x,z} D_{x,z} + \beta_{x,z} D_{x,z}'$ with $\delta(\Delta p/p) = \delta p/p$ as the reference momentum stays constant when the beam is not accelerated. We have neglected the time variation of the synchrotron frequency during the collision. From now on the short notation $\eta \overset{\text{def}}{=} \Delta p/p$ will be used.

To calculate the mean value of the emittance and momentum deviation change for one particle, we have to average with respect to the second particle betatron angles and momentum deviations. Therefore, to get the overall mean value of the emittance and momentum deviation changes for all particles, we have to average further with respect to all betatron angles, momentum deviations and positions of the first particle. This means that we have to integrate over all phase space volume V of betatron coordinates, momentum deviations and azimuthal positions of two interacting particles, using a probability density function P for the betatron amplitudes and angles, momentum deviations and azimuthal positions of the interacting particles:

$$\left\langle \frac{d}{d\bar{t}} \frac{\langle \varepsilon_{x_1} \rangle}{\beta_x} \right\rangle = \int_{\bar{V}} 2c\bar{\beta}\, \bar{P} d\bar{V} \int_{\bar{\psi}_{min}}^{\pi} d\bar{\psi} \int_0^{2\pi} d\bar{\phi}\, \bar{\sigma}(\bar{\psi}) \sin\bar{\psi} \frac{\delta\varepsilon_{x_1}}{\beta_x}, \tag{6}$$

where the outer and inner brackets denote the average value over the ring optical parameters and the average over the particle beam. An overhead bar symbol refers to the CM frame. Here, $\bar{\sigma}(\bar{\psi})d\bar{\Omega}$ is the Coulomb scattering cross-section in the CM frame for a scattering event into a solid angle $d\bar{\Omega}(\bar{\psi},\bar{\phi}) = \sin\bar{\psi}\, d\bar{\psi} d\bar{\phi}$. The time intervals in CM and LAB frames are $d\bar{t}$ and dt $(dt = \gamma d\bar{t})$, c is the speed of light, $2c\bar{\beta}$ is the relative velocity of two interacting particles in the CM frame and P is a probability density function of 12 phase space variables for the particle pair in the LAB frame (and $\bar{P} = P/\gamma$ in CM). P reduces to 9 variables as $s_1 = s_2$ and $x_{\beta_1} + D_x\eta_1 = x_{\beta_2} + D_x\eta_2$ (idem for $z_{\beta_{1,2}}$) since the positions the particles are supposed to remain constant during the collision, i.e.

$$\begin{aligned} P &\overset{12\text{var}}{\Longleftrightarrow} P_{\eta s}(\eta_1, s_1) P_{\eta s}(\eta_2, s_2) P_{x_\beta x'_\beta}(x_{\beta_1} x'_{\beta_1}) P_{x_\beta x'_\beta}(x_{\beta_2} x'_2) P_{z_\beta z'_\beta}(z_{\beta_1} z'_{\beta_1}) P_{z_\beta z'_\beta}(z_{\beta_2} z'_{\beta_2}), \\ P &\overset{9\text{var}}{\Longleftrightarrow} P_\eta(\eta_1) P_\eta(\eta_2) P_s(s_1) P_{x_\beta}(x_{\beta_1}) P_{x'_\beta}(x'_{\beta_1}) P_{x'_\beta}(x'_{\beta_2}) P_{z_\beta}(z_{\beta_1}) P_{z'_\beta}(z'_{\beta_1}) P_{x'_\beta}(z'_{\beta_2}). \end{aligned} \tag{7}$$

2.4.2.2 *Averaging over the Scattering Angles and All Particles*

Using the "classical" Rutherford differential cross-section $\sigma(\bar{\psi})$ the likelihood of a collision per unit time and solid angle element $d\bar{\phi}$ in CM frame, denoted P_{scat}, is determined by the particle density distribution in phase space P (LAB frame). Since $2\bar{\beta}c$ is the relative velocity between two colliding particles we can write

$$P_{\text{scat}}(\bar{\psi},\bar{\phi},P) = \frac{2\bar{\beta}cP\sigma(\bar{\psi})d\bar{\Omega}}{\gamma^2}, \quad \bar{\sigma}(\bar{\psi})d\bar{\Omega} = \frac{r_{\text{i}}^2}{16\bar{\beta}^4 \sin^4[\frac{\bar{\psi}}{2}]} \sin\bar{\psi}\, d\bar{\psi} d\bar{\phi}, \quad r_{\text{i}} = \frac{e^2Z^2}{4\pi\epsilon_0 mc^2 A}, \tag{8}$$

r_i is the classical ion radius in SI units, with the ion mass and charge A, Z, relative to proton or the electron mass m and electron charge e (the second γ^2 comes from an "underlying" time interval $d\bar{t} = dt/\gamma$). Let us mention that for non-relativistic collisions the maximum impact parameter $\bar{b}_{\max}$ gives a cut-off value $\bar{\psi}_{\min}$ for the scattering angle, $\bar{C}_{\log}$ is the "Coulomb logarithm":

$$\tan\frac{\bar{\psi}_{\min}}{2} \approx \frac{r_i}{2\bar{\beta}^2\bar{b}_{\max}}, \text{ if } \bar{\psi}_{\min} \ll 1: \quad \bar{C}_{\log} \overset{\text{def}}{=} \log\frac{\bar{b}_{\max}}{\bar{b}_{\min}} \approx \log\frac{2}{\bar{\psi}_{\min}} \approx \log\frac{2\bar{\beta}^2\bar{b}_{\max}}{r_{\text{i}}}. \tag{9}$$

In the LAB frame $b_{\max} = \bar{b}_{\max}$ and the Coulomb logarithm is defined alike $C_{\log} \approx \log\frac{2\beta^2 b_{\max}}{r_{\text{i}}}$. For example, integrating $\langle \delta H_1 \rangle/\gamma^2$ over $\bar{\phi}$ and $\bar{\psi}$ gives with Eq. (9)

$$\int_{\bar{\psi}_{min}}^{\pi} d\bar{\psi} \int_0^{2\pi} d\bar{\phi}\, \bar{\sigma}(\bar{\psi}) \sin\bar{\psi} \left\{\frac{\delta H_1}{\gamma^2}\right\} = \frac{\pi r_i^2}{4\bar{\beta}^4} \log\left[\frac{2\bar{\beta}^2 \bar{b}_{max}}{r_{\mathrm{i}}}\right] \left\{-\frac{4\eta_1}{\gamma}\xi + \theta^2 + \zeta^2\right\}. \quad (10)$$

At this stage we make the following ad-hoc change of phase space variables, in conformity with Eq. (2), to compute the mean change of the invariants $\varepsilon_{x,z}$ and H. Here, the density distribution P transforms into $\mathcal{P}$, using new variables including the angles ξ, θ, ζ:

$$P(\eta_1, \eta_2, s_1, x_{\beta_1}, x'_{\beta_1}, x'_{\beta_2}, z_{\beta_1}, z'_{\beta_1}, z'_{\beta_2}) \longmapsto \mathcal{P}(\eta, \xi, s, x_\beta, x'_\beta, \theta, z_\beta, z'_\beta, \zeta), \quad (11)$$

$$\begin{aligned} x_{\beta_{1,2}} &= x_\beta \mp \frac{D_x \gamma \xi}{2}, \quad x'_{\beta_{1,2}} = x'_\beta \pm \frac{\theta - D'_x \gamma \xi}{2}, \quad \eta_{1,2} = \eta \pm \frac{\gamma\xi}{2}, \\ z_{\beta_{1,2}} &= z_\beta \mp \frac{D_z \gamma \xi}{2}, \quad z'_{\beta_{1,2}} = z'_\beta \pm \frac{\zeta - D'_z \gamma \xi}{2}, \quad \eta_{1,2} = \eta \pm \frac{\gamma\xi}{2}. \end{aligned} \quad (12)$$

Obviously, $\mathcal{P}$ is symmetric with respect to ξ, θ, ζ and thus the integrals vanish for the linear terms in ξ, θ, ζ of the integrands. Then, keeping only the factors ξ^2, θ^2, ζ^2 and using the variables $\eta, \xi, s, x_\beta, x'_\beta, \theta, z_\beta, z'_\beta, \zeta$ defined in Eqs. (11-12) to integrate the three invariants (see Eq. (6)) yields Eq. (12), where the phase space volume element expressed in the new variables is $d\mathcal{V} = d\eta d\xi ds dx_\beta dx'_\beta d\theta dz_\beta dz'_\beta d\zeta$:

$$\left\langle \frac{d}{dt} \begin{bmatrix} \langle H \rangle / \gamma^2 \\ \langle \varepsilon_x \rangle / \beta_x \\ \langle \varepsilon_z \rangle / \beta_z \end{bmatrix} \right\rangle = \frac{\pi c r_{\mathrm{i}}^2}{2} \int_{\mathcal{V}} \frac{d\mathcal{V}}{\bar{\beta}^3 \gamma} \mathcal{P}(\eta, s, \xi, x_\beta, x'_\beta, \theta, z_\beta, z'_\beta) \log\left[\frac{2\bar{\beta}^2 \bar{b}_{\max}}{r_{\mathrm{i}}}\right]$$
$$\begin{Bmatrix} \theta^2 + \zeta^2 - 2\xi^2 \\ \xi^2 + \zeta^2 - 2\theta^2 + \frac{D_x^2 + \widetilde{D}_x^2}{\beta_x^2}\gamma^2(\theta^2 + \zeta^2) - \frac{2\gamma_x D_x^2}{\beta_x}\gamma^2\xi^2 - \frac{2D'_x}{\beta_x}\left(\alpha_x D_x + \widetilde{D}_x\right)\gamma^2\xi^2 \\ \xi^2 + \theta - 2\zeta^2 + \frac{D_z^2 + \widetilde{D}_z^2}{\beta_z^2}\gamma^2(\theta^2 + \zeta^2) - \frac{2\gamma_z D_z^2}{\beta_z}\gamma^2\xi^2 - \frac{2D'_z}{\beta_z}\left(\alpha_z D_z + \widetilde{D}_z\right)\gamma^2\xi^2 \end{Bmatrix}. \quad (13)$$

This formula for the mean change of the invariants makes no supposition about the distribution $\mathcal{P}$ of particles in the bunch. Therefore, the integral can be in principle computed for arbitrary probability laws. However, since "Gaussian integration" is easily performed, many analytical IBS models are based on Gaussian distributions.

So, we use here bi-Gaussian density distributions for the betatron amplitudes and angles $P_{x_\beta x'_\beta}(x_{\beta_{1,2}}, x'_{\beta_{1,2}})$, $P_{z_\beta z'_\beta}(z_{\beta_{1,2}}, z'_{\beta_{1,2}})$ and the momentum and bunch length $P_{\eta s}(\eta_{1,2}, s_{1,2})$. Also, to shorten the formalism and obtain manageable formulae we will neglect the derivatives of the dispersion and transverse betatron functions:

$$D'_{x,z} = 0, \quad \beta'_{x,z} = -2\alpha_{x,z} = 0, \quad \widetilde{D}_{x,z} = \alpha_{x,z} D_{x,z} + \beta_{x,z} D'_{x,z} = 0, \quad \gamma_{x,z} = \frac{1}{\beta_{x,z}}. \quad (14)$$

Then, with the change of variables (Eq. (12)), we rewrite the Gaussian distributions in terms of the nine new variables, $\eta, s, \xi, x_\beta, x'_\beta, \theta, z_\beta, z'_\beta, \zeta$:

$$\begin{gathered} \mathcal{P}_{x_\beta x'_\beta}\left(x_\beta \mp \frac{D_x \gamma \xi}{2}, x'_\beta \pm \frac{\theta}{2}\right), \quad \mathcal{P}_{z_\beta z'_\beta}\left(z_\beta \mp \frac{D_z \gamma \xi}{2}, z'_\beta \pm \frac{\zeta}{2}\right), \\ \mathcal{P}_\eta\left(\eta \pm \frac{\gamma\xi}{2}\right), \quad \mathcal{P}_s(s). \end{gathered} \quad (15)$$

After integration of the distribution $\mathcal{P}$ over the 6 variables $x_\beta, x'_\beta, z_\beta, z'_\beta, \eta, s$, we get:

$$\mathcal{P}(\xi,\theta,\zeta) \equiv N_b \prod_{u=x_\beta,x'_\beta}^{\eta,s} \int_{-\infty}^{\infty} \mathcal{P}_u du$$
$$= \frac{\mathcal{A}\beta^3\gamma^4}{c r_i^2 \pi} \exp\left[-\frac{\gamma^2\xi^2}{4}\left(\frac{1}{\sigma_\eta^2}+\frac{D_x^2}{\sigma_{x\beta}^2}+\frac{D_z^2}{\sigma_{z\beta}^2}\right)-\frac{\theta^2}{4\sigma_{x'_\beta}^2}-\frac{\zeta^2}{4\sigma_{z'_\beta}^2}\right], \quad (16)$$
$$\mathcal{A} = \frac{c r_i^2 N_b}{64\pi^2\beta^3\gamma^4\sigma_{x_\beta}\sigma_{x'_\beta}\sigma_{z_\beta}\sigma_{z'_\beta}\sigma_\eta\sigma_s} = \frac{c r_i^2 N_b}{64\pi^2\beta^3\gamma^4\varepsilon_x\varepsilon_z\varepsilon_s},$$

where N_b is the number of particles in the bunch, $\varepsilon_s = \sigma_\eta\sigma_s$ and $\varepsilon_{x,z} = \sigma_{x_\beta,z_\beta}^2/\beta_{x,z} \equiv \sigma_{x'_\beta,z'_\beta}^2\beta_{x,z}$ are the longitudinal and transverse rms emittances. Assuming non-relativistic particle velocities in the CM frame, we express β in LAB frame by means of a momentum-energy Lorentz transformation from CM to LAB. We obtain (Ref. [1]):

$$\bar{\beta} \approx \frac{\beta\gamma}{2}\sqrt{\left(\frac{\eta_1-\eta_2}{\gamma}\right)^2+(x'_1-x'_2)^2+(z'_1-z'_2)^2} = \frac{\beta\gamma}{2}\sqrt{\xi^2+\theta^2+\zeta^2}. \quad (17)$$

Finally, it remains to transform the change of momenta and energy for the two colliding particles back to the LAB frame, replacing $\bar{\beta}$ by its approximation Eq. (17). Let us define the parameter $q = \gamma\sqrt{2\beta^2 b_{\max}/r_i}$. Since $D'_{x,z} = \alpha_{x,z} = 0$ we can rework Eq. (13) this way:

$$\left\langle \frac{d}{dt}\begin{bmatrix}\langle H\rangle/\gamma^2\\ \langle\varepsilon_x\rangle/\beta_x\\ \langle\varepsilon_z\rangle/\beta_z\end{bmatrix}\right\rangle = 4\mathcal{A}\iiint_{-\infty}^{\infty}\exp\left[-\frac{\gamma^2\xi^2}{4}\left(\frac{1}{\sigma_\eta^2}+\frac{D_x^2}{\sigma_{x\beta}^2}+\frac{D_z^2}{\sigma_{z\beta}^2}\right)-\frac{\theta^2}{4\sigma_{x'_\beta}^2}-\frac{\zeta^2}{4\sigma_{z'_\beta}^2}\right]$$
$$\begin{Bmatrix}\theta^2+\zeta^2-2\xi^2\\ \xi^2+\zeta^2-2\theta^2+\frac{D_x^2}{\beta_x^2}\gamma^2(\theta^2+\zeta^2-2\xi^2)\\ \xi^2+\theta-2\zeta^2+\frac{D_z^2}{\beta_z^2}\gamma^2(\theta^2+\zeta^2-2\xi^2)\end{Bmatrix}\log\left[\frac{q^2}{4}(\xi^2+\theta^2+\zeta^2)\right]\frac{d\xi d\theta d\zeta}{\xi^2+\theta^2+\zeta^{2\,3/2}} \quad (18)$$

The remaining three integrals still need to be computed to get the mean change of the invariants. To this end, let us do a first change of variables $\xi,\theta,\zeta \to 2(u,v,w)/q$ to transform Eq. (18) to the coordinates (u,v,w), followed, by a second spherical-like change of variables $(u,v,w) \to \sqrt{r}(\sin\mu\cos\nu, \sin\mu\sin\nu, \cos\mu)$. This trick will allow us to derive the IBS growth rates in a synchrotron after some more approximations.

2.4.2.3 *Calculation of Rise Times Neglecting $\alpha_{x,z}$ and $D'_{x,z}$*

The IBS growth rates can be expressed in the form

$$\frac{1}{T_\eta} = \frac{1}{\sigma_\eta}\frac{d\sigma_\eta}{dt} \equiv \frac{1}{2\langle H\rangle}\frac{d\langle H\rangle}{dt}, \quad \frac{1}{T_{x,z}} = \frac{1}{\sigma_{x_\beta z_\beta}}\frac{d\sigma_{x_\beta z_\beta}}{dt} \equiv \frac{1}{2\langle\varepsilon_{x,z}\rangle}\frac{d\langle\varepsilon_{x,z}\rangle}{dt}, \quad (19)$$

where T_η, T_x and T_z are the longitudinal, horizontal, and vertical IBS rise times, and $H = \eta^2$, supposing negligible synchrotron frequency values (i.e. $\Omega_s \approx 0$) for the duration of a particle-pair collision. Evidently, the time derivatives of $\langle H\rangle/\gamma^2$ and $\langle\varepsilon_{x,z}\rangle/\beta_{x,z}$ in Eq. (18) have to

be revisited to match the growth rate definition. For this, let us define the following parameters and functions [6]

$$\frac{1}{\sigma_h^2}=\frac{1}{\sigma_\eta^2}+\frac{D_x^2}{\sigma_{x_\beta}^2}+\frac{D_z^2}{\sigma_{z_\beta}^2},\quad \sigma_h^2=\frac{\sigma_\eta^2\sigma_{x_\beta}^2}{D_x^2\sigma_\eta^2+\sigma_{x_\beta}^2\left[1+\left(\frac{D_z\sigma_\eta}{\sigma_{z_\beta}}\right)^2\right]}\overset{D_z=0}{\Longrightarrow}\sigma_h=\frac{\sigma_\eta\sigma_{x_\beta}}{\sigma_x},$$

$$a=\frac{\sigma_h}{\gamma\sigma'_{x_\beta}}\equiv\frac{\sigma_h}{\gamma}\sqrt{\frac{\varepsilon_x}{\beta_x}}\overset{D_z=\alpha_{x,z}=0}{\Longrightarrow}a=\frac{\beta_x\sigma_\eta}{\gamma\sigma_x},\quad b=\frac{\sigma_h}{\gamma\sigma'_{z_\beta}}\equiv\frac{\sigma_h}{\gamma}\sqrt{\frac{\varepsilon_z}{\beta_z}}\overset{D_z=\alpha_{x,z}=0}{\Longrightarrow}b=\frac{\beta_z\sigma_\eta}{\gamma\sigma_z},\qquad(20)$$

$$c=q\sigma_h=\left(\gamma\sqrt{\frac{2\beta^2 b_{\max}}{r_{\mathrm{i}}}}\right)\sigma_h\overset{\text{Eq.9}}{\Longleftrightarrow}\gamma\exp\left[\frac{C_{\log}}{2}\right]\sigma_h,$$

$$\begin{gathered}D(\mu,\nu)=\frac{1}{c^2}\left(b^2\cos^2\mu+\sin^2\mu\left(\cos^2\nu+a^2\sin^2\nu\right)\right),\\ g_1(\mu,\nu)=1-3\sin^2\mu\cos^2\mu\quad g_2(\mu,\nu)=1-3\sin^2\mu\sin^2\mu,\\ g_3(\mu,\nu)=1-3\cos^2\mu,\end{gathered}\qquad(21)$$

where $C_{\log}$ is the Coulomb logarithm (cf. Eq. (9)). Thus Eq. (19) can be written

$$\begin{bmatrix}1/T_\eta\\1/T_x\\1/T_z\end{bmatrix}=\left\langle\frac{q^2}{2c^2}\begin{bmatrix}\sigma_h^2/\sigma_\eta^2\\a^2\\b^2\end{bmatrix}\frac{d}{dt}\begin{bmatrix}\langle H\rangle/\gamma^2\\\langle\varepsilon_x\rangle/\beta_x\\\langle\varepsilon_z\rangle/\beta_z\end{bmatrix}\right\rangle=\frac{\mathcal{A}}{c^2}\int_0^\infty dr\int_0^\pi d\mu\int_0^{2\pi}d\nu$$
$$\times\sin\mu\exp[-rD(\mu,\nu)]\log[r]\begin{Bmatrix}\frac{\sigma_h^2}{\sigma_\eta^2}g_1(\mu,\nu)\\a^2g_2(\mu,\nu)+\frac{D_x^2\sigma_h^2}{\beta_x\varepsilon_x}g_1(\mu,\nu)\\b^2g_3(\mu,\nu)+\frac{D_z^2\sigma_h^2}{\beta_z\varepsilon_z}g_1(\mu,\nu)\end{Bmatrix}\qquad(22)$$

We can rewrite a more compact form of Eq. (22), replacing the 3 functions g_i by the "scattering function" $f(a,b,c)$, where $\rho{=}r/c^2$ replaces r and adding the function D_0:

$$D_0(\mu,\nu)=\sin^2\mu\left(a^2\cos^2\nu+b^2\sin^2\nu\right)+\cos^2\mu,\qquad(23)$$

$$\begin{gathered}f(a,b,c)=2\int_0^\pi d\mu\int_0^{2\pi}d\nu\sin\mu\left(1-3\cos^2\mu\right)\\ \times\int_0^\infty d\rho\log[c^2\rho]\exp[-\rho D_0(\mu,\nu)].\end{gathered}\qquad(24)$$

The integral over ρ can be solved analytically:

$$\int_0^\infty d\rho\log[c^2\rho]\exp[-\rho D_0(\mu,\nu)]=\frac{-C_{\mathrm{Euler}}+2\log c-\log[D_0(\mu,\nu)]}{D_0(\mu,\nu)},\qquad(25)$$

were $C_{\mathrm{Euler}}{\approx}0.5772$ is Euler's constant. From Eq. (20), we get $\log c^2=C_{\log}+\log[\gamma^2{\sigma_h}^2]\approx C_{\log}$ assuming that $C_{\log}{\gg}\log[\gamma^2{\sigma_h}^2]$. This sounds fine as in most cases $10{\lesssim}C_{\log}{\lesssim}20$ (e.g. for the LHC: $\gamma{=}7000$, $\sigma_\eta{\approx}10^{-4}$, $C_{\log}{\approx}20$, and with $\sigma_h{\approx}\sigma_\eta$ we get $\log[c^2]\approx C_{\log}\gg\log\left[\gamma^2{\sigma_\eta}^2\right]=-0.7$). The remaining variables μ,ν are then transformed into $x{=}\cos\mu$, $z{=}2\nu$ using symmetry properties of trigonometric functions. Hence, using Eq.

(25), f can be reduced to a single integral (see Ref. [7]) and cast into the form (with $\tilde{C}=2\log c - C_{\text{Euler}}$):

$$f(a,b,c) = 8\pi \int_0^1 dx \left(2\log\left[\frac{\tilde{C}}{2}\left\{\frac{1}{\sqrt{P(x)}}+\frac{1}{\sqrt{Q(x)}}\right\}\right] - C_{\text{Euler}}\right)\frac{1-3y^2}{\sqrt{P(y)Q(y)}}, \qquad (26)$$
$$P(y) = a^2 + (1-a^2)y^2 \quad Q(y) = b^2 + (1-b^2)y^2.$$

After some work, the IBS growth rates for bunched beams (Eq. 22) are written as in [6]-[9]:

$$\begin{pmatrix} \frac{1}{T_\eta} \\ \frac{1}{T_x} \\ \frac{1}{T_z} \end{pmatrix} = \mathcal{A} \begin{pmatrix} \left\langle \frac{\sigma_h^2}{\sigma_\eta^2} f(a,b,c) \right\rangle \\ \left\langle f\left(\frac{1}{a},\frac{b}{a},\frac{c}{a}\right) + \frac{D_x^2\sigma_h^2}{\beta_x\varepsilon_x} f(a,b,c) \right\rangle \\ \left\langle f\left(\frac{1}{b},\frac{a}{b},\frac{c}{b}\right) + \frac{D_z^2\sigma_h^2}{\beta_z\varepsilon_z} f(a,b,c) \right\rangle \end{pmatrix}. \qquad (27)$$

The first term in each transverse growth rate of Eq. (27) corresponds to a straight excitation of their own emittance. Each of the second term relates to the longitudinal growth rate T_η^{-1} and to the dispersion $D_{x,z}^2$ that possibly makes a coupling of the longitudinal growth into their respective transverse planes.

Many storage rings are planar (with reference orbit in the median plane (s,x) i.e. zero vertical dispersion D_z=0). So, Eq. (26) shortens to (with $1 - D_x^2\sigma_\eta^2/\sigma_x^2 = \sigma_h^2/\sigma_\eta^2$):

$$\begin{pmatrix} \frac{1}{T_\eta} \\ \frac{1}{T_x} \\ \frac{1}{T_z} \end{pmatrix} = \mathcal{A} \begin{pmatrix} \left\langle \left[1 - \frac{D_x^2\sigma_\eta^2}{\sigma_x^2}\right] f(a,b,c) \right\rangle \\ \left\langle f\left(\frac{1}{a},\frac{b}{a},\frac{c}{a}\right) + \frac{D_x^2\sigma_\eta^2}{\sigma_x^2} f(a,b,c) \right\rangle \\ \left\langle f\left(\frac{1}{b},\frac{a}{b},\frac{c}{b}\right) \right\rangle \end{pmatrix}, \qquad (28)$$

which is the original IBS Piwinski's formula [1]. As the growth times change with the momentum spread (square) η^2 and the emittances $\varepsilon_{x,z}$, an iterative procedure is needed to compute the evolution of growth time, and so update η^2 and $\varepsilon_{x,z}$ (cf. last chapter).

2.4.2.4 *Invariant*

In the presence of IBS, bunched beams may experience phase space dilution leading to continuous growth of the momentum spread and/or growth of one or both transverse emittances. The performance of the beam can be described via an invariant that is arranged in a form close to the sum of the mean value of the change in emittance and that in momentum deviation due to the particle collisions (supposing $H=\eta^2$).

$$\left(\frac{1}{\gamma^2} - \left\langle\frac{D_x^2}{\beta_x^2}\right\rangle - \left\langle\frac{D_z^2}{\beta_z^2}\right\rangle\right)\eta^2 + \left\langle\frac{1}{\beta_x}\right\rangle\varepsilon_x + \left\langle\frac{1}{\beta_z}\right\rangle\varepsilon_z = \text{constant}. \qquad (29)$$

Each term on the left hand side of Eq. (29) is positive in case the coefficient of η^2 is positive. So, the sum of the three positive invariants, and thus of the three oscillation energies, is limited and the beam can attain an equilibrium (i.e. the IBS emittance growth is bounded). In case the coefficient of η^2 is negative the total oscillation energy can increase

as long as it does not exceed further limitations. Then, no beam equilibrium can exist. Noting that, unlike planar rings, the conditions for beam equilibrium do not depend whether the storage rings are below or above the transition.

For planar rings with $D_z = 0$ the latter formula can be rewritten, assuming the "smooth focusing approximation" holds, as:

$$\left(\frac{1}{\gamma^2} - \frac{1}{\gamma_t^2}\right)\eta^2 + \left\langle\frac{1}{\beta_x}\right\rangle \varepsilon_x + \left\langle\frac{1}{\beta_z}\right\rangle \varepsilon_z = \text{constant},$$
$$\langle D_x\rangle \equiv \frac{R}{Q_x^2}, \quad \alpha_p = \left\langle\frac{D_x(s)}{\rho(s)}\right\rangle \equiv \frac{1}{\gamma_t^2}, \quad \eta_t = \frac{1}{\gamma_t^2} - \frac{1}{\gamma^2}, \tag{30}$$

where γ_t is the transition energy, α_p the momentum compaction factor, η_t the slip factor and Q_x the machine tune. As a result, below the transition ($\eta_t<0$) the coefficient of η^2 is positive and the beam can reach an equilibrium. Above transition ($\eta_t\geq 0$) the coefficient of η^2 is negative and the beam cannot reach an equilibrium.

Figure 2 shows an application of the Piwinski's IBS model to the "Extra low energy antiproton" synchrotron (ELENA ≈ 30 m circumference). ELENA is a below transition ring with $\eta_t \approx -0.72$ (for $\gamma \approx 1$ at 100 keV), designed to decelerate antiprotons at 5.31 MeV kinetic energy (100 MeV/c) sent by the Antiproton Decelerator (AD), to yield dense beams at 100 keV (13.7 MeV/c). ELENA cycle with electron-cooling plateaus and deceleration ramps is overlaid to the plot.

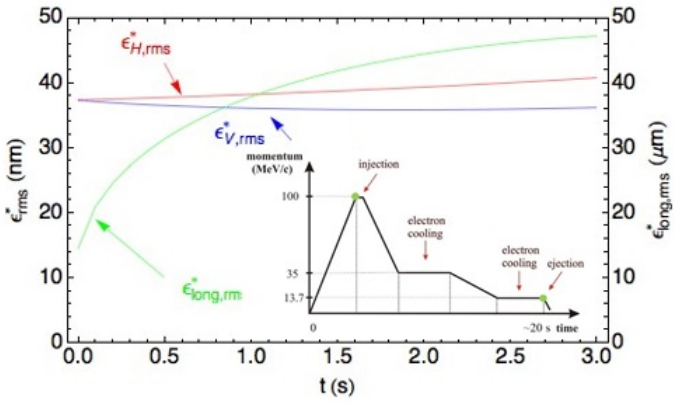

Figure 2: Antiproton deceleration down the 3s ELENA second ramp, from 0.65 MeV (35 MeV/c) to 100 keV, after the second cooling plateau. Initial rms emittances are $\varepsilon^*_{x,z} = 37.3$ nm (physical emittances $\varepsilon_{x,z} = 1\ \mu$m), $\varepsilon^*_s = 14.4$ nm (or $\varepsilon^*_s = 0.56\ meVs$). The emittance evolution is calculated with IBS, by iteratively re-evaluating the growth rates, as they are determined by the emittance values, and since the energy decreases versus time. With regard to the plot, there is no strong argument to discard slow deceleration ramps between plateaus with electron cooling. (*Mathematica* code written by C. Carli, with linear coupling).

2.4.3 **Bjorken-Mtingwa Model**

2.4.3.1 ***Beam Phase Space Density and Invariants***

The IBS model formulated as in [2], in line with the work of Piwinski [1], considers Gaussian laws for the beam density distributions in phase space:

$$P(\vec{r},\vec{p}) = \frac{N_b}{\Gamma}\exp[S(\vec{r},\vec{p})], \quad \Gamma = \int \exp[S(\vec{r},\vec{p})]\, d^3\vec{r}d^3\vec{p},$$
$$S(\vec{r},\vec{p}) = \frac{1}{2}\sum_{i,j=1}^{3}\left(A_{ij}\delta p_i\delta p_j + B_{ij}\delta p_i\delta r_j + C_{ij}\delta r_i\delta r_j\right) = S^{(x)} + S^{(z)} + S^{(s)}, \quad (31)$$

where $P(\vec{r},\vec{p})$ is the phase space density of a beam holding N_b particles, Γ is the phase beam space volume and $S(\vec{r},\vec{p})$ is the Gaussian particle beam density distribution, $\delta\vec{r}$ and $\delta\vec{p}$ are the position and momentum from the reference values $\vec{r}$ and $\vec{p}$. Working out the coefficients A_{ij} , B_{ij} and C_{ij}, the particle beam density distribution can be written

$$S^{(x)} = \frac{\beta_x}{2\sigma_{x_\beta}^2}\left(\gamma_x x_\beta^2 + 2\alpha_x x_\beta x'_\beta + \beta_x x'^2_\beta\right),$$
$$S^{(z)} = \frac{\beta_z}{2\sigma_{z_\beta}^2}\left(\gamma_z z_\beta^2 + 2\alpha_z z_\beta z'_\beta + \beta_z z'^2_\beta\right), \quad S^{(s)} = \frac{\eta^2}{2\sigma_\eta^2} + \frac{\eta(s-s_0)^2}{2\sigma_\eta^2}. \quad (32)$$

Like in Eq. (16) $\varepsilon_s{=}\sigma_\eta\sigma_s$ and $\varepsilon_{x,z}{=}\sigma_{x_\beta,z_\beta}^2/\beta_{x,z}{\equiv}\sigma_{x'_\beta,z'_\beta}^2\beta_{x,z}$ are the longitudinal and transverse emittances and $\sigma_{\eta,}\sigma_s, \sigma_{x,z}, \sigma'_{x,z}$ the rms momentum spread, length, width and height of a bunch beam.

2.4.3.2 *Two-Body Scattering: Rate of Change of Emittances and Momentum*

Unlike Piwinski, the approach to IBS of Bjorken and Mtingwa is based on the time-evolution operator « S-matrix » that relates transitions from an initial quantum state $|i\rangle$ to a final state $|f\rangle$ of a physical system experiencing a scattering process. The matrix elements of S are inner products symbolized $\langle f|S|i\rangle$. The S-matrix is proportional to the amplitude $\mathcal{M}$ that represents the physics of the interaction process.

Following [2] (see also [4], where they proceed through a slightly different way) the "transition rate" for a two-particle scattering process, namely the number of scattering events per unit time, is given by Ref. [10]:

$$\frac{\mathrm{d}\wp}{dt} = \frac{1}{2}\int d^3\vec{r}\,\frac{d^3\vec{p}_1}{\gamma_1}\frac{d^3\vec{p}_2}{\gamma_2}\,P(\vec{r},\vec{p}_1)\,P(\vec{r},\vec{p}_2)|\mathcal{M}|^2\,\frac{d^3\vec{p}'_1}{\gamma'_1}\frac{d^3\vec{p}'_2}{\gamma'_2}\frac{\delta^4(\vec{p}_1+\vec{p}'_2-\vec{p}'_1-\vec{p}_2)}{(2\pi)^2}, \quad (33)$$

where a prime $'$ refers to the particle parameters after collision, $\gamma_{1,2}{=}E_{1,2}/m$, $E_{1,2}$ are the two colliding particle' energy (in Heaviside Lorentz units in which $\epsilon_0{=}\hbar{=}c{=}1$), m their mass and $\mathcal{M}$ is the Coulomb "scattering amplitude" of a particle-pair collision. Then, using the beam density distribution $S(\vec{r},\vec{p})$ allows to compute the rate of change of the emittances ε_u $(u{=}x,z,s)$; we obtain:

$$\frac{\mathrm{d}\varepsilon_u}{dt} = \frac{1}{2\Gamma^2}\int d^3\vec{r}\,\frac{d^3\vec{p}_1}{\gamma_1}\frac{d^3\vec{p}_2}{\gamma_2}\exp[-S(\vec{r},\vec{p}_1)]\,P(\vec{r},\vec{p}_1)\,P(\vec{r},\vec{p}_2)$$
$$\times\,|\mathcal{M}|^2(\varepsilon_u(\vec{p}_1) - \varepsilon_u(\vec{p}'_1) + \varepsilon_u(\vec{p}'_2) - \varepsilon_u(\vec{p}_2))\,\frac{d^3\vec{p}'_1}{\gamma'_1}\frac{d^3\vec{p}'_2}{\gamma'_2}\frac{\delta^4(\vec{p}_1+\vec{p}'_2-\vec{p}'_1-\vec{p}_2)}{(2\pi)^2}. \quad (34)$$

The aim is to compute the scattering amplitude $\mathcal{M}$. This will be done by means of the "Feynman rules", using the "Feynman diagram" representation of a scattering process stemming from quantum electrodynamic theory (Ref. [10]):

$$|\mathcal{M}|^2 = \frac{e^4}{\vec{p}^4\sin^4[\psi/2]}. \quad (35)$$

At this point the calculations are still far from finished, and also they are not easy to perform. After some difficult manipulations the rate of change of the emittances $\mathrm{d}\varepsilon_u/dt$, can be recast in the form given by Eq. (36) below. See [2] for details of the rather lengthy calculations required to derive the following Bjorken–Mtingwa growth rates.

2.4.3.3 *Intrabeam Scattering Growth Rates*

The formula for the IBS growth rates derived by the Bjorken-Mtingwa formalism are:

$$\frac{1}{T_u} = \frac{\mathrm{d}\log\varepsilon_u}{dt} = \frac{\pi^2 N_b c r_\mathrm{i}^2 C_\mathrm{log}}{\gamma\Gamma}\left\langle \int_0^\infty d\lambda \sqrt{\frac{\lambda}{\det[L+\lambda \mathrm{I}]}}\left\{\mathrm{Tr}[L_u]\mathrm{Tr}\left[\frac{1}{L+\lambda\mathrm{I}}\right] - 3\mathrm{Tr}\left[\frac{1}{L_u+\lambda\mathrm{I}}\right]\right\}\right\rangle, \quad (36)$$

with

$$\Gamma = (2\pi)^2(\beta\gamma)^3\varepsilon_x\varepsilon_z\sigma_\eta\sigma_s = (2\pi)^2(\beta\gamma)^3\varepsilon_x\varepsilon_z\varepsilon_s, \quad (37)$$

$$L_x = \frac{\beta_x\gamma^2}{\varepsilon_x}\begin{bmatrix} \frac{1}{\gamma^2} & -\frac{\phi_x}{\gamma} & 0 \\ -\frac{\phi_x}{\gamma} & \frac{H_x}{\beta_x} & 0 \\ 0 & 0 & 0 \end{bmatrix}, \quad L_z = \frac{\beta_z\gamma^2}{\varepsilon_z}\begin{bmatrix} 0 & 0 & 0 \\ 0 & \frac{H_z}{\beta_z} & -\frac{\phi_z}{\gamma} \\ 0 & -\frac{\phi_z}{\gamma} & \frac{1}{\gamma^2} \end{bmatrix}, \quad L_s = \frac{\gamma^2}{\sigma_\eta^2}\begin{bmatrix} 0 & 0 & 0 \\ 0 & 1 & 0 \\ 0 & 0 & 0 \end{bmatrix}, \quad (38)$$

$$\phi_{x,z} = \frac{D_{x,z}\alpha_{x,z} + D'_{x,z}\beta_{x,z}}{\beta_{x,z}}, \quad H_{x,z} = \frac{D_{x,z}\alpha_{x,z} + \beta_{x,z}^2\phi_{x,z}^2}{\beta_{x,z}}. \quad (39)$$

In Eq. (36) the Coulomb logarithm C_log is defined in Refs. [2,5,8] in terms of the maximum and minimum impact parameters and minimum scattering angle. Diverse definitions for C_log exist. Luckily, its logarithmic dependence means that it varies slowly over a large range of the parameters involved in its definition (e.g. Eq. (9)). Ref. [2] takes the fixed Coulomb logarithm C_log=20. Also, c is the speed of light, r_i is the classical ion radius, $\vec{p}$ and E_0 the particle momentum rest energy, and γ=$\sqrt{E_0^2 + p^2}/E_0$. The matrices inside the brackets depend on the emittances, momentum spread and bunch length (with ε_s=$\sigma_\eta\sigma_s$ in m). For matched beams the longitudinal emittance is defined as ε_s=$\pi p\sigma_\eta\sigma_s\beta^{-1}c^{-1}$ in eVs. After expansion of the integrand in the brackets of Eq. (36) and some lengthy computations, the growth rates are finally stated in the form given in Ref. [3], with u=x, z, s:

$$\frac{1}{T_u} = \frac{\pi^2 N_b c r_i^2 C_\mathrm{log}}{\gamma\Gamma}\Delta_u\left\langle \int_0^\infty d\lambda \frac{\sqrt{\lambda}(a_u\lambda + b_u)}{(\lambda^3 + a\lambda^2 + b\lambda + c)^{3/2}}\right\rangle, \quad \Delta_x = \frac{\gamma^2 H_x}{\varepsilon_x}, \quad \Delta_z = \frac{\gamma^2 H_z}{\varepsilon_z}, \quad \Delta_s = \frac{\gamma^2}{\sigma_\eta}. \quad (40)$$

The nine coefficients $a, b, c, a_x, b_x, a_z, b_z, a_s, b_s$ depend on the optics parameters. They are not reproduced here (cf. Ref. [3] for the full list). The Bjorken-Mtingwa IBS growth rates seem somewhat dissimilar from the ones in the Piwinski formulae. However, the two groups of formulae match fairly well with certain approximations. In Ref. [4], Kubo, Mtingwa and Wolski develop the high-energy approximation "Completely integrated modified Piwinski" (CIMP) which shows an asymptotic equivalence with the Bjorken-Mtingwa growth rates formulae.

2.4.4 **Zenkevich Model**

Other IBS models based on non-Gaussian distributions have been formulated using the kinetic analysis for the modelling of small angle multiple Coulomb scattering. The method exposed here is based on the solution of the Fokker–Planck equation (FPE) for the particle density distribution, expressed in the position-momentum phase space. The FPE is an integro-differential equation with friction and diffusion coefficients with account of the multiple IBS.

Here, we summarize the approach developed by Zenkevich, to solve the FPE using Monte Carlo tool for IBS simulations in three degrees of freedom by means of a macro-particle algorithm called "binary collision map" (BCM) and realized in the macro-particle code "Monte-Carlo code" (MOCAC) for numerical modelling of IBS effects in accelerators and storage rings. Afterwards, another macro-particle code called "Software for Intrabeam Scattering and Radiation Effects" (SIRE) was developed to simulate the evolution of beam particle distributions in storage rings, taking into account IBS, radiation damping and quantum excitation. MOCAC and SIRE are both tracking codes where the beam is represented by a large number of macro-particles occupying points in the six-dimensional position-momentum phase space.

2.4.4.1 ***Fokker–Planck Formalism***

The evolution of the particle distribution in a non-equilibrium beam facing to multiple micro Coulomb scattering can be expressed by the Fokker–Planck approach, where the collision term considers the many interactions between the charged particles as a series of small-angle scatterings. Assume that we know how to find a function $P(\vec{u}, \Delta\vec{u})$ such that it represents the conditional transition probability of a change in momentum $\vec{u}$ to $\vec{u} \to \vec{u} - \Delta\vec{u}$ in time Δt of a particle in an individual collision. Hence, the time evolution of the position-momentum distribution $f(\vec{r}, \vec{u}, t)$ of particles in phase space is (Eq. (41) shows in what manner $f(\vec{r}, \vec{u}, t)$ happens to be just how it is at time t as a result of how it was at an earlier time $t - \Delta t$):

$$f(\vec{r}, \vec{u}, t) = \int f(\vec{r}, \vec{u} - \Delta\vec{u}, t - \Delta t) P(\vec{u} - \Delta\vec{u}, \Delta\vec{u}) d\Delta\vec{u}\,, \quad \int P(\vec{u}, \Delta\vec{u}) d\Delta\vec{u} = 1, \qquad \iint_{|\vec{r}|^3 |\vec{u}|^3} f(\vec{r}, \vec{u}, t) d\vec{r} d\vec{u} = N. \tag{41}$$

N is the number of particles in the whole or a part of the beam, $d\vec{w} \overset{\text{def}}{=} d|\vec{w}|^3$ and $d\vec{r} \overset{\text{def}}{=} d|\vec{r}|^3$ are the momentum and space volume elements and $|\vec{r}|^3 |\vec{u}|^3$ indicates the phase space volume to integrate; $\vec{u}$ and $\vec{r}$ will be well-defined later (Eq. (46)). Truly f could just be thought as a momentum distribution of $\vec{u}$ and t, but keeping $\vec{r}$ offers flexibilities.

Multiple small-angle scattering is dominant in IBS process where $\Delta\vec{u}$ is small for small Δt. This allows expanding in Taylor' series, to first order in Δt and second order in $\Delta\vec{u}$ the product fP inside the integral:

$$\begin{aligned} f(\vec{r}, \vec{u} - \Delta\vec{u}, t - \Delta t) P(\vec{u} - \Delta\vec{u}, \Delta\vec{u}) &\approx f(\vec{r}, \vec{u}, t) P(\vec{u}, \Delta\vec{u}) \\ -\Delta t \frac{\partial}{\partial t} [f(\vec{r}, \vec{u}, t) P(\vec{u}, \Delta\vec{u})] - \Delta\vec{u} \cdot \frac{\partial}{\partial \vec{u}} [f(\vec{r}, \vec{u}, t) P(\vec{u}, \Delta\vec{u})] & \\ + \frac{1}{2} \sum_{i,j} \Delta u_i \Delta u_j \frac{\partial^2}{\partial u_i \partial u_j} [f(\vec{r}, \vec{u}, t) P(\vec{u}, \Delta\vec{u})] & \end{aligned} \tag{42}$$

Inserting this result in $f(\vec{r},\vec{u},t)$ (Eq. (41)) yields (integrations over momentum volumes):

$$\begin{aligned} f(\vec{r},\vec{u},t) = f(\vec{r},\vec{u},t)\int P(\vec{u},\Delta\vec{u})d\Delta\vec{u} - \Delta t\frac{\partial f(\vec{r},\vec{u},t)}{\partial t}\int P(\vec{u},\Delta\vec{u})d\Delta\vec{u} \\ -\int \Delta\vec{u}\cdot\frac{\partial}{\partial\vec{u}}\left[f(\vec{r},\vec{u},t)P(\vec{u},\Delta\vec{u})\right]d\Delta\vec{u} \\ +\frac{1}{2}\int\sum_{i,j}\frac{\partial^2}{\partial u_i\partial u_j}\left[f(\vec{r},\vec{u},t)\Delta u_i\Delta u_j P(\vec{u},\Delta\vec{u})\right]d\Delta\vec{u} \end{aligned} \quad (43)$$

Then, P is normalized to one and f does not depend on $\Delta\vec{u}$, Eq.(43) transforms into the rate of change of the density distribution $f(\vec{r},\vec{u},t)$ for any momentum $\vec{u}=(u_x,u_y,u_z)$ (subscripts x,y,z refer to the momentum directions, i,j stand for x,y,z):

$$\frac{\partial f(\vec{r},\vec{u},t)}{\partial t} = -\frac{\partial}{\partial\vec{u}}\cdot\left[f(\vec{r},\vec{u},t)\frac{\langle\Delta\vec{u}\rangle}{\Delta t}\right] + \frac{1}{2}\sum_{i,j}\Delta u_i\Delta u_j\frac{\partial^2}{\partial u_i\partial u_j}\left[f(\vec{r},\vec{u},t)\frac{\langle\Delta u_i\Delta u_j\rangle}{\Delta t}\right]. \quad (44)$$

The quantities $\langle\Delta\vec{u}\rangle \overset{i=x,y,z}{\Longleftrightarrow} \langle\Delta u_i\rangle$ and $\langle\Delta u_i\Delta u_j\rangle$ are the mean changes in $\Delta\vec{u}$ and $\Delta u_i\Delta u_j$ in time Δt as a result of scattering events, that is the first and mixed moments of the transition probability function $P(\vec{u},\Delta\vec{u})$, referred to as $\vec{F}$ and D_{ij}:

$$\vec{F} \overset{\text{def}}{=} \left\langle\frac{\Delta\vec{u}}{\Delta t}\right\rangle = \int\frac{\Delta\vec{u}}{\Delta t}P(\vec{u},\Delta\vec{u})\,d\Delta\vec{u}, \quad D_{ij} \overset{\text{def}}{=} \frac{1}{2}\left\langle\frac{\Delta u_i\Delta u_j}{\Delta t}\right\rangle = \frac{1}{2}\int\frac{\Delta u_i\Delta u_j}{\Delta t}P(\vec{u},\Delta\vec{u})\,d\Delta\vec{u}. \quad (45)$$

The two collision terms $\langle\Delta\vec{u}\rangle/\Delta t$ and $\langle\Delta u_i\Delta u_j\rangle/\Delta t$ characterize a "frictional dynamic" and a "diffusion in momentum space", with opposite sign in Eq. (44), which may be in balance for an equilibrium. Inserting $\vec{F}$ and D_{ij} in Eq. (44) results in the compact formulation:

$$\frac{\partial f}{\partial t} = -\frac{\partial}{\partial\vec{u}}\cdot\left(\vec{F}f\right) + \sum_{i,j}\frac{\partial^2}{\partial u_i\partial u_j}\left(D_{ij}f\right). \quad (46)$$

The transport process Eqs. (44-46) is the Fokker-Planck equation (Refs. [16]-[17]). To solve it one must specify $P(\vec{u},\Delta\vec{u})$ to get $\langle\Delta\vec{u}\rangle$. Yet, there is an indirect way to do it. Suppose that multiple collisions are handled as series of particle-pair collisions, then, the mean momentum changes $\langle\Delta\vec{u}\rangle$ and $\langle\Delta u_i\Delta u_j\rangle$ are computable via the Coulomb scattering cross-section (since $\langle\Delta\vec{u}\rangle$ contains the physics of the scattering process via Eq. (48) below).

Let us work out the friction $\vec{F}$ and diffusion D_{ij} terms. For this purpose, we explore the different ways collisions are able to change the momentum of a "test" particle in a time Δt, and average all the occurrences of $\Delta\vec{u}$ and $\Delta u_i\Delta u_j$. For ease, this will first be resolved in the CM frame and then converted back to the LAB frame (if wanted). The incidence of collisions in time Δt on a test particle is evaluated for a certain "field" particle momentum by averaging $\Delta\vec{u}$ on all possible factors that affect $\Delta\vec{u}$ (i.e. azimuthal and scattering angles in IBS events). Next, averaging is computed for all field particle momenta $\vec{w}$ via the density distribution $f(\vec{r},\vec{w},t)$. Just after collisional time interval Δt, each field particle momentum is replaced by $\vec{w}\to\vec{w}+\Delta\vec{w}\equiv\vec{w}^{\star}$ (the sign $\star$ refer to post collision momenta).

2.4.4.2 *Single Pair-Collision Event*

In the framework of particle-pair collision events, let us define the position $\vec{r}$ and dimensionless momentum $\vec{P}$ vectors for a test particle $\vec{u}$ and a field particle $\vec{w}$ as:

$$\vec{r} = (z - z_s, x, y), \quad \vec{P} = \left(\frac{\eta}{\gamma} \overset{\text{def}}{=} \frac{1}{\gamma}\frac{\Delta p}{p}, x' \overset{\text{def}}{=} \frac{p_x}{p}, y' \overset{\text{def}}{=} \frac{p_y}{p}\right) = \begin{cases} \vec{u} & \text{test particle} \\ \vec{w} & \text{field particle} \end{cases}. \quad (47)$$

The vectors $(\vec{r}, \vec{u})$ are the phase space coordinates, where z is the longitudinal deviation of a moving particle about the design orbit, with respect to the bunch centre z_c and x, y are the horizontal and vertical deviations of that particle in a plane perpendicular to the design orbit. In addition, η, x', y' are the relative longitudinal and transverse momenta, assuming a constant reference particle momentum p. The kinematics of the relative momentum changes after a pair collision between particles $\vec{u}$ and $\vec{w}$ in transverse and longitudinal directions are taken from the Piwinski model Eq. (1), with $\Delta\vec{u}=\Delta u_x\hat{x}+\Delta u_y\hat{y}+\Delta u_z\hat{z}$:

$$\Delta\vec{u} = \vec{u}^\star - \vec{u} = \begin{cases} \frac{1}{2}\left[\frac{U_y U \sin\bar{\phi} - U_z U_x \cos\bar{\phi}}{U_\perp}\sin\bar{\psi} + U_x(\cos\bar{\psi} - 1)\right] \\ \frac{1}{2}\left[\frac{U_x U \sin\bar{\phi} - U_z U_y \cos\bar{\phi}}{U_\perp}\sin\bar{\psi} + U_y(\cos\bar{\psi} - 1)\right], \\ \frac{1}{2}[U_\perp \cos\bar{\phi}\sin\bar{\psi} + U_z(\cos\bar{\psi} - 1)] \end{cases} \quad (48)$$

where

$$\vec{U} = \vec{u} - \vec{w} = (U_z, U_x, U_y), \quad U_\perp = \sqrt{U_x^2 + U_y^2},$$
$$U = |\vec{U}| = \sqrt{U_z^2 + U_x^2 + U_y^2} = |\vec{u} - \vec{w}| = \sqrt{\frac{(\eta_u - \eta_w)^2}{\gamma^2} + (x'_u - x'_w)^2 + (y'_u - y'_w)^2}, \quad (49)$$

in which $\bar{\psi}$ and $\bar{\phi}$ are the scattering and azimuthal angles in the centre of mass frame (CM). For elastic collisions we have $\Delta\vec{w} = -\Delta\vec{u}$, namely $\vec{u}^\star - \vec{u} = \vec{w}^\star - \vec{w}$ or $\vec{u}^\star - \vec{w}^\star = \vec{u} - \vec{w}$. Figure 3 pictorially displays the kinematic of a collision between a pair of particles with momenta $\vec{u}$ and $\vec{w}$ in the centre of mass of the particles, using the notation in Eqs. (47-49).

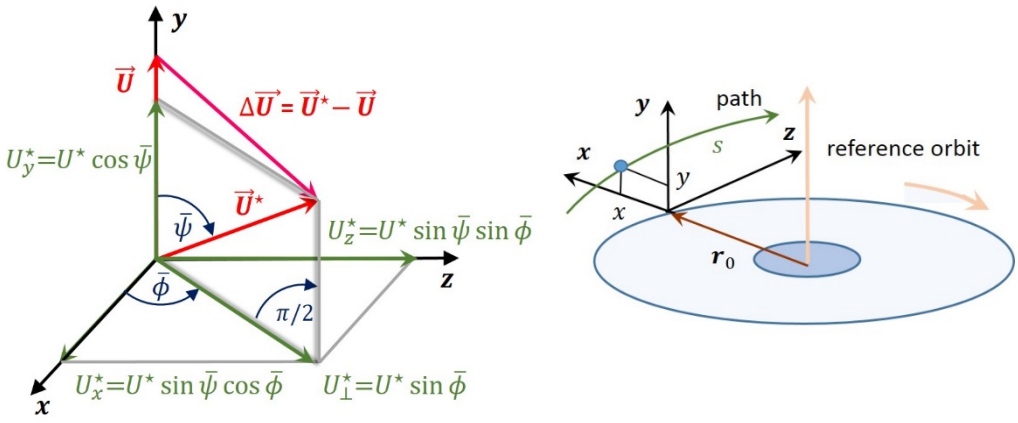

Figure 3: Left figure: Binary collision in the CM frame. Before collision, the two particles, with momenta $\vec{u}$ and $\vec{w}$, move non-relativistically in opposite direction parallel to the vertical y-axis.

Relative particle momenta $\vec{U}=\vec{u}\text{-}\vec{w}$ before and after collision are outlined. The reference trihedral is such that before collision $\vec{U}$ lays on the y-axis i.e. $\vec{U}=|\vec{u}\text{-}\vec{w}|\hat{y}$, and is perpendicular to the longitudinal z-axis of the reference orbit (the hat means unit vector). After collision $\vec{U}^{\star}=\vec{u}^{\star}\text{-}\vec{w}^{\star}=U_x^{\star}\hat{x}+U_y^{\star}\hat{y}+U_z^{\star}\hat{z}$; likewise $\Delta\vec{U}=\vec{U}^{\star}\text{-}\vec{U}=\Delta\vec{u}\text{-}\Delta\vec{w}$. So with the momenta shown in the sketch we get the result $\Delta\vec{U}/U=\sin\bar{\psi}\cos\bar{\phi}\,\hat{x}+\left(\cos\bar{\phi}\text{ -}1\right)\hat{y}+\sin\bar{\psi}\sin\bar{\phi}\,\hat{z}$, since $\vec{\mathrm{U}}\|\hat{\mathrm{y}}$. Right figure: Frenet-Seret curved coordinate system in a storage ring, with the reference orbit and an individual particle trajectory. The particle location is: $r(s)=r_0(s)+x(s)\hat{x}+y(s)\hat{y}$.

As a primary step to evaluate the change in particle momentum change let us average $\Delta\vec{u}(\bar{\psi},\bar{\phi})$ over the angle $\bar{\phi}$ only by way of Eq. (48), that is not including the scattering angle $\bar{\psi}$. We then obtain:

$$\langle\Delta\vec{u}\rangle_{\phi}=\frac{1}{2\pi}\int_0^{2\pi}\Delta\vec{u}\,\sin\bar{\psi}\,d\bar{\phi}=-\sin^2\frac{\bar{\psi}}{2}(\vec{u}-\vec{w}), \tag{50}$$

in which integrating $\Delta\vec{u}$ gives the vector $-\sin^2\psi/2\,\{U_z,U_x,U_y\}$, from which the above average follows since $\vec{U}=\vec{u}-\vec{w}$. We will use this result later. Now, to find the momentum mean changes during particle-pair collisions because of IBS we use the expression P_{scat} to quantify the chance of collisions per unit time (in CM frame, with the a solid angle element $d\bar{\Omega}=\sin\bar{\psi}\,d\bar{\psi}d\bar{\phi}$):

$$P_{\mathrm{scat}}(\vec{r},\vec{u},\bar{\psi},\bar{\phi},t)=\frac{2\bar{\beta}cf(\vec{r},\vec{u},t)\bar{\sigma}(\bar{\psi})d\bar{\Omega}}{\gamma^2},\quad \bar{\sigma}(\bar{\psi})=\left(\frac{r_{\mathrm{i}}}{4\bar{\beta}^2\sin^2\left[\frac{\bar{\psi}}{2}\right]}\right)^2. \tag{51}$$

The density distribution $f(\vec{r},\vec{u},t)$ is defined in LAB frame and $\sigma(\bar{\psi})$ is the Rutherford cross-section (Eq. (8)). In analogy with Eq. (46), the FPE in phase space relevant to study the beam evolution in storage rings attributable to IBS effects is

$$\frac{\partial}{\partial t}f(\vec{r},\vec{u},t)=-\frac{\partial}{\partial\vec{u}}\cdot\left[\vec{F}\,f(\vec{r},\vec{u},t)\right]+\sum_{i,j}\frac{\partial^2}{\partial u_i\partial u_j}\left[D_{ij}\,f(\vec{r},\vec{u},t)\right], \tag{52}$$

in which the summation is made over repeating indices. The frictional and diffusion coefficients are definite in terms of averaged scattering events, noting that $P_{\mathrm{scat}}(\vec{r},\vec{u},\bar{\psi},t)$ acts for the transition probability $P(\vec{u},\Delta\vec{u})$ used in Eq. (45):

$$\begin{aligned}\vec{F}&\equiv\left\langle\frac{\Delta\vec{u}}{\Delta t}\right\rangle_{\vec{w}}=\int\frac{\Delta\vec{u}}{\Delta t}P_{\mathrm{scat}}(\vec{r},\vec{u},\bar{\psi},t)\,d\vec{u},\\ D_i&\equiv\frac{1}{2}\left\langle\frac{\Delta u_i\Delta u_j}{\Delta t}\right\rangle_{\vec{w}}=\frac{1}{2}\int\frac{\Delta u_i\Delta u_j}{\Delta t}P_{\mathrm{scat}}(\vec{r},\vec{u},\bar{\psi},t)\,d\vec{u}.\end{aligned} \tag{53}$$

Then, using $\Delta\vec{u}\overset{\text{def}}{=}\Delta u_{\iota}=\left(\Delta u_x,\Delta u_y,\Delta u_z\right)$ (cf. Eq. (48)), the average $\langle\Delta\vec{u}\rangle_{\vec{w}}$ of $\Delta\vec{u}$ for a test particle (in CM frame) is computed in two steps: the first average, named $\langle\Delta\vec{u}\rangle_{\phi\psi}$, integrate $\Delta\vec{u}$ on all possible azimuthal and scattering angles $\bar{\phi}$, $\bar{\psi}$; the second average, named $\langle\langle\Delta\vec{u}\rangle_{\phi\psi}\rangle_{\vec{w}}$, integrate $\langle\Delta\vec{u}\rangle_{\phi\psi}$ over all field particles $\vec{w}$ with phase space distribution $f(\vec{r},\vec{u},t)$ (for shortness $\langle\langle\Delta\vec{u}\rangle_{\phi\psi}\rangle_{\vec{w}}$) is renamed $\langle\Delta\vec{u}\rangle_{\vec{w}}$ hereinafter). The result of double integration is:

$$\begin{aligned}\langle\Delta\vec{u}\rangle_{\phi\psi} &= \int_{\bar{\psi}_{\min}}^{\pi}\int_0^{2\pi}\Delta\vec{u}\,P_{\text{scat}}d\bar{\phi}d\bar{\psi} = -\frac{\pi c r_{\text{i}}^2}{\bar{\beta}^3\gamma^2}\log\left[\frac{2\bar{\beta}^2\bar{b}_{\max}}{r_{\text{i}}}\right](\vec{u}-\vec{w}),\\ \langle\Delta\vec{u}\rangle_{\vec{w}} &\overset{\text{def}}{=} \int_{|\vec{w}|^3}\langle\Delta\vec{u}\rangle_{\phi\psi}\,f(\vec{r},\vec{w},t)d\vec{w} = \rho_r(\vec{r},t)\int_{|\vec{w}|^3}\langle\Delta\vec{u}\rangle_{\phi\psi}\,\tilde{f}(\vec{r},\vec{w},t)d\vec{w}\\ &= -\left\langle\frac{\pi c r_i^2\rho(\vec{r},t)}{\bar{\beta}^3\gamma^2}\log\left[\frac{2\bar{\beta}^2\bar{b}_{\max}}{r_{\text{i}}}\right](\vec{u}-\vec{w})\right\rangle_{\vec{w}},\\ \rho_r(\vec{r},t) &\overset{\text{def}}{=} \int_{|\vec{w}|^3}f(\vec{r},\vec{w},t)d\vec{w}\,,\quad \tilde{f}(\vec{r},\vec{w},t) = f(\vec{r},\vec{w},t)/\rho_r(\vec{r},t),\end{aligned} \tag{54}$$

where $\langle\cdot\rangle_{\vec{w}}$ means averaging over the field particles $\vec{w}$, $\rho_r(\vec{r},t)$ is the distribution in position coordinates after integration of $f(\vec{r},\vec{w},t)$ over $d\vec{w}$, and $\tilde{f}(\vec{r},\vec{w},t)$ is the local distribution in momentum coordinates for a given $\vec{r}$. Therefore, integrating $\rho_r(\vec{r},t)$ over $d\vec{r}$ yields the number N of particles in the bunch, like integrating $f(\vec{r},\vec{w},t)$ over $d\vec{r}d\vec{w}$ (Eq. (41)). Differently the integral of $\tilde{f}(\vec{r},\vec{w},t)$ over $d\vec{r}d\vec{w}$ is unity. By way of Eq. (17) the Lorentz factor $\bar{\beta}$ in CM converts to $\bar{\beta}\approx\beta\gamma|\vec{u}-\vec{w}|/2$ in LAB; so, the first moments are:

$$\langle\Delta\vec{u}\rangle_{\vec{w}} = -\left\langle\frac{\pi c r_{\text{i}}^2\rho_r(\vec{r},t)}{\beta^3\gamma^2}\bar{C}_{\log}\right\rangle_{\vec{w}},\quad \langle\Delta\vec{u}\rangle_{\vec{w}} = -\left\langle\frac{8\pi c r_{\text{i}}^2\rho_r(\vec{r},t)}{\beta^3\gamma^5}C_{\log}(\vec{u},\vec{w})\frac{\vec{u}-\vec{w}}{|\vec{u}-\vec{w}|^3}\right\rangle_{\vec{w}}, \tag{55}$$

in which $\bar{C}_{\log}$ is the CM frame Coulomb logarithm and $C_{\log}(\vec{u},\vec{w})$ is the "extended" Coulomb logarithm defined in LAB frame:

$$\bar{C}_{\log} = \log\left[\frac{2\bar{\beta}^2 b_{\max}}{r_{\text{i}}}\right],\quad C_{\log}(\vec{u},\vec{w}) = \log\left[\frac{\beta^2\gamma^2 b_{\max}}{2r_{\text{i}}}(\vec{u}-\vec{w})^2\right]. \tag{56}$$

We proceed similarly to compute the second moments in LAB frame by computing the averages of $\Delta\vec{u}\,\Delta\vec{u}\overset{\text{def}}{=}\Delta u_i\Delta u_j=\left(\Delta u_x\Delta u_x,\Delta u_x\Delta u_y\ldots\Delta u_z\Delta u_z\right)$. The result is:

$$\langle\Delta u_i\Delta u_j\rangle_{\vec{w}} \approx \left\langle\frac{4\pi c r_i^2\rho_r(\vec{r},t)}{\beta^3\gamma^5}C_{\log}(\vec{u},\vec{w})\frac{\delta_{ij}|\vec{u}-\vec{w}|^2-(u_i-w_i)(u_j-w_j)}{|\vec{u}-\vec{w}|^3}\right\rangle_{\vec{w}}, \tag{57}$$

where $\delta_{ij}=1$ if $i=j$, $\delta_{ij}=0$ if $i\neq j$ is the Kronecker symbol.

The study of the beam evolution in phase space of the distribution $f(\vec{r},\vec{u},t)$ demands in theory to solve a kinetic equation such as FPE (Eq. (52)) including the computation of $\vec{F}$ and D_{ij} by integration of $f(\vec{r},\vec{u},t)$ as shown in the above three formulae. If one might solve the FPE, the knowledge of particle positions and momenta resulting from the phase space density $f(\vec{r},\vec{u},t)$ would give the progression of longitudinal and transverse beam emittances caused by multiple particle-pair collisions inside the beam. Yet in practice the FPE is complicated to solve in both the six and three-dimensional forms. Instead, we consider a different technique using macro-particles for IBS simulation, founded on the Zenkevich "binary collision map" (BCM).

2.4.4.3 *Monte Carlo Binary Collision Model*

The BCM is an algorithm that allows to "reduce" the effects of the continuous time dynamical IBS system to a discrete time "map" in momentum space. Indeed, BCM, replaces a multiple scattering process acting in a time gap Δt by a discrete set of binary collision events. This method operates on each pair of macro-particles and calculates the change of momenta during a collision event (shown through the angles ψ and ϕ). The BCM algorithm

first proceeds by sampling at random macro-particle pairs $(\vec{u}^i, \vec{w}^j)$ for approximate the continuous densities $\tilde{f}(\vec{r}, \vec{u}, t)$ and $\rho_r(\vec{r}, t)$ in Eq. (54), that are now changed to the discrete distributions $\tilde{f}_N(\vec{r}, \vec{u}, t)$ and $\rho_N(\vec{r}, t)$, formally written as:

$$\tilde{f}_N(\vec{r}, \vec{u}, t) = \frac{1}{N}\sum_{i=1}^{N} \delta(\vec{r} - \vec{r}^i)\,\delta(\vec{u} - \vec{u}^i), \quad \rho_N(\vec{r}, t) = \int_{|\vec{u}|^3} f_N(\vec{r}, \vec{u}, t) d\vec{u},$$
$$\iint_{|\vec{r}|^3 |\vec{u}|^3} \tilde{f}_N(\vec{r}, \vec{u}, t) d\vec{r} d\vec{u} = 1, \quad \int_{|\vec{r}|^3} \rho_N(\vec{r}, t) d\vec{u} = \mathrm{N}, \tag{58}$$

where δ is the Dirac delta function, and the superscripts i, j stand for a macro-particle numbers. N is either the number of macro-particles populating a 6-D phase space or a 3-D spatial volume. By means of the discretization procedure the macro-particles $\vec{r}^i$, $\vec{u}^i$ can be grouped into an input "list" and identified by their 6-D position-momentum vectors. We assume the functions $\tilde{f}_N$ and ρ_N remain stable during the interaction time Δt and that a given macro-particle in the list collides only once. So $\tilde{f}_N = \tilde{f}_N(\vec{r}, \vec{u})$ and $\rho_N = \rho_N(\vec{r})$ are time-independent. Observing the mean momentum changes $\langle \Delta\vec{u} \rangle_\phi$ in Eq. (50) and $\langle \Delta\vec{u} \rangle_{\phi\psi}$ in Eq. (54) show that they are similar providing the scattering angle $\bar{\psi}^{ij}$ or ψ^{ij} (CM/LAB frames) is defined as follows and the azimuthal angle $\bar{\phi}^{ij}$ or ϕ^{ij} is randomly chosen in the interval $[0, 2\pi]$ (see Refs. [11-13]). For shortness, we add the coefficients:

$$\bar{A}_0 = \frac{\pi c r_\mathrm{i}^2}{\bar{\beta}^3 \gamma^2}, \quad A_0 = \frac{8\pi c r_\mathrm{i}^2}{\beta^3 \gamma^5}.$$

Hence:

$$\sin\left[\frac{\bar{\psi}^{ij}}{2}\right] = \sqrt{\bar{A}_0 \rho_N(\vec{r}) \log\left[\frac{2\bar{\beta}^2 b_{\max}}{r_\mathrm{i}}\right] \Delta t}, \quad \sin\left[\frac{\bar{\psi}^{ij}}{2}\right] = \sqrt{\bar{A}_0 \rho_N(\vec{r}) \bar{C}_{\log}\, \Delta t},$$
$$\sin\left[\frac{\psi^{ij}}{2}\right] = \sqrt{A_0 \frac{\rho_N(\vec{r}) \log\left[\frac{\beta^2 \gamma^2 b_{\max}}{2 r_\mathrm{i}} |\vec{u}^i - \vec{w}^j|^2\right] \Delta t}{|\vec{u}^i - \vec{w}^j|^3}}, \quad \sin\left[\frac{\psi^{ij}}{2}\right] = \sqrt{A_0 \frac{\rho_N(\vec{r}) C_{\log}[\vec{u}^i, \vec{w}^j] \Delta t}{|\vec{u}^i - \vec{w}^j|^3}}. \tag{59}$$

The time interval Δt in the formula acts to fit the units as $\langle \Delta\vec{u} \rangle_{\vec{w}}$ is in 1/s while $\langle \Delta\vec{u} \rangle_\phi$ has no unit. In addition, Δt is the time step of a collisional cycle, supposed short enough for noticeable variation of beam momenta and $\Delta t \ll T_{z,x,y}$ the IBS rise times. The maximum impact parameter $b_{\max}$ is taken as the beam height or half the beam diameter, $\rho_N(\vec{r})$ is the discrete particle density.

The BCM algorithm first divides the N macro-particle domain representing the beam into "cells" with equal volume; then, it groups at random all the macro-particles into $N/2$ pairs and distributes the pairs in the cells to form a discrete macro-particle density distribution as illustrated in Fig. 4.

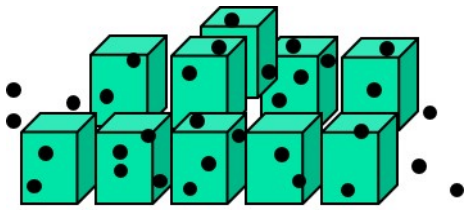

Figure 4: Pictorial representation of the macro-particle domain split into cells with macro-particles grouped at random within the cells. Each pair of macro-particles picked undertakes a single collision within the duration Δt of an interaction cycle.

Clearly the 3-D macro-particle distribution $\rho_N(\vec{r},t)$ for the total or a fraction of the beam also applies to macro-particle distributions in little cell volumes. Let us assume that the density inside each cell is uniform and that two colliding macro-particles in the same cell have an equal spatial location. Note that the macro-particle positions, namely longitudinal and transverse displacements about the design orbit remain unchanged through the collision mapping. To simulate real IBS effects we must adjust the cell density $\rho_N(\vec{r},t)$ to the number of real particles (i.e. macro-particles × particle number per macro-particle). For suitability, the "scattering angle" $\bar{\psi}^{ij}$ in every pair of macro-particles in each cell is chosen to refer to the CM frame (Eq. (59) upper formula).

The collisional simulation is realized by a recurrent mapping procedure, that is we insert $\vec{u}^i$, $\vec{w}^i$ and $\sin\bar{\phi}^{ij}$, $\cos\bar{\psi}^{ij}$ onto the Piwinski's formula (Eq. (48)), which returns $\Delta\vec{u}^i$ and $\Delta\vec{w}^i$ for each pair $\{\vec{u}^i,\vec{w}^j\}$ within the cycle time Δt. So the post collisional momenta are $\vec{u}^{i\star}=\vec{u}^i+\Delta\vec{u}^i$ and $\vec{w}^{i\star}=\vec{w}^i+\Delta\vec{w}^i$. After each cycle, in every cell the momentum distribution is updated for all macro-particle pair as $\{\eta^{i\star},x'^{i\star},y'^{i\star}\}=\{\eta^i+\Delta\eta^i,\ x'^i+\Delta x'^i,\ y'^i+\Delta y'^i\}$, where $\{\Delta\eta'^i,\Delta x'^i,\Delta y'^i\}$ stands for both $\vec{u}^i$ and $\vec{w}^i$. A new cycle of length Δt is next started until the end of the simulation time. Once a cycle is over the post collision macro-particle invariants ε_z^i (for bunched beams), ε_x^i and ε_y^i are upgraded. They are derived from the following expressions:

$$\begin{aligned}
\varepsilon_z^i &= \gamma_z\left(\Delta z^i\right)^2, \quad \gamma_z \overset{\text{def}}{=} \frac{\nu_s^2}{\eta_t^2 R^2},\\
\varepsilon_x^i &= \gamma_x\left(x^i - D_x\eta^i\right)^2 + 2\alpha_x\left(x^i - D_x\eta^i\right)\left(x'^i - D_x'\eta^i\right) + \beta_x\left(x'^i - D_x'\eta^i\right)^2, \\
\varepsilon_y^i &= \gamma_y\left(y^i - D_y\eta^i\right)^2 + 2\alpha_y\left(x^i - D_y\eta^i\right)\left(y'^i - D_y'\eta^i\right) + \beta_y\left(y'^i - D_y'\eta^i\right)^2,
\end{aligned} \tag{60}$$

where $\nu_s=|\Omega_s|/\omega_0$ is the synchrotron tune, Ω_s the synchrotron frequency, ω_0 the revolution frequency, η_t the slip factor and R the mean storage ring radius; $\alpha_{x,y},\beta_{x,y},\gamma_{x,y}$ are the Twiss parameters and $D_{x,y},D'_{x,y}$ the dispersion functions and their derivatives varying, along the reference orbit . Inversely related, the particle phase space positions and momentum coordinates $\Delta z^i,x^i,y^i$, and η^i,x'^i,y'^i are stated by means of the invariants and phases $\phi_{z,y,x}$:

$$\frac{\Delta p^i}{p}=\eta^i=-\sqrt{\frac{\varepsilon_z^i}{\beta_z}}(\alpha_z\cos\phi_z+\sin\phi_z)=-\sqrt{\frac{\varepsilon_z^i}{\beta_z}}\sin\phi_z,\qquad z^i\text{-}z_s^i=\Delta z^i=\sqrt{\beta_z\,\varepsilon_z^i}\cos\phi_z\,,$$
$$\frac{p_x^i}{p}=x'^i=-\sqrt{\frac{\varepsilon_x^i}{\beta_x}}(\alpha_x\cos\phi_x+\sin\phi_x)+D_x'\eta^i,\qquad x^i=\left(\beta_x\,\varepsilon_x^i\right)^{1/2}\cos\phi_x+D_x\eta^i,\quad(61)$$
$$\frac{p_y^i}{p}=y'^i=-\sqrt{\frac{\varepsilon_y^i}{\beta_y}}\left(\alpha_y\cos\phi_y+\sin\phi_y\right)+D_y'\eta^i,\qquad y^i=\left(\beta_y\,\varepsilon_y^i\right)^{1/2}\cos\phi_y+D_y\eta^i,$$

where $\beta_z\overset{\text{def}}{=}\frac{|\eta_t|R}{\nu_s}=$constant, which implies that $\alpha_z\overset{\text{def}}{=}-\frac{\beta_z'}{2}\equiv 0$ (Ref. [5]).

- In the binary collision method implemented in MOCAC and SIRE tracking codes, the macro-particle beam is a set of 6-D position-momentum vectors. An initial macro-particle density distribution is generated by sampling a Gaussian probability law. Extra selective laws with non-Gaussian tails can be added if needed. Anyhow, at the beginning of the simulation the initial distribution must reflect the Courant-Snyder and longitudinal invariants of the beam.
- Non-uniform synchrotron lattices are modelled as series of sets attached to the optical parameters located at separate azimuthal "points" around a lattice period; and, then averaged over the period. The mapping is reiterated all the way in each cell, through every time step Δt, in different points of the lattice period.

Now combining all macro-particles within a bunch, we can compute the average values of the individual invariants $\varepsilon_{z,x,y}^i$ around the ring by means of Eq. (60) and considering the variations of the Twiss parameters and dispersion functions with their derivatives. Lastly, the longitudinal, horizontal and vertical IBS growth rates write:

$$\varepsilon_{z,x,y}=\langle\varepsilon_{z,x,y}^i\rangle,\quad\frac{1}{T_{z,x,y}}=\frac{1}{\sqrt{\varepsilon_{z,x,y}}}\frac{d\sqrt{\varepsilon_{z,x,y}}}{dt}=\frac{1}{2\varepsilon_{z,x,y}}\frac{d\varepsilon_{z,x,y}}{dt}.\qquad(62)$$

2.4.5 **Benchmarking of the IBS Theoretical Models with Monte-Carlo Codes**

The IBS theoretical models have been studied in detail and benchmarked with experimental data for hadron beams over the years [18, 19]. In hadron machines, the IBS effect causes emittance dilution with time, limiting their performance. Lepton machines on the other hand, were operating until today in regimes were the IBS effect was negligible. Future linear collider Damping Rings, new generation light sources and B-factories, however, enter in regimes where the IBS effect can be predominant. It is thus important to study the IBS theories in the presence of synchrotron radiation damping (SRD) and quantum excitation (QE), benchmark the existing theoretical models and tracking codes with experimental data and identify their limitations. Even though *e+/e−* rings run normally above transition, where IBS leads to continuous emittance growth and equilibrium does not exist, synchrotron radiation damping counteracts the IBS growth, leading to new steady-state emittances. The beam transverse emittance and relative energy spread evolution due to the effects of IBS and SRD can be obtained by solving numerically the three coupled differential equations:

$$\frac{d\varepsilon_i}{dt} = -\frac{2}{\tau_i}(\varepsilon_i - \varepsilon_{i0}) + \frac{2\varepsilon_i}{T_i(\varepsilon_x,\varepsilon_y,\sigma_p)}, i = x, y,$$
$$\frac{d\sigma_p}{dt} = -\frac{1}{\tau_p}(\sigma_p - \sigma_{p0}) + \frac{\sigma_p}{T_p(\varepsilon_x,\varepsilon_y,\sigma_p)}, \quad (63)$$

using small time iteration steps δt which are much smaller than the damping time and for which the emittances change adiabatically. The symbols ε_{x0}, ε_{y0}, σ_{p0} denote the zero-current (without the effect of IBS) equilibrium horizontal and vertical emittances and rms energy spread. τ_x, τ_y, τ_p are the synchrotron radiation damping times. From the IBS growth times T_x, T_y, T_p, one can obtain the steady state properties, for which: $\frac{d\varepsilon_x}{dt} = \frac{d\varepsilon_y}{dt} = \frac{d\sigma_p^2}{dt} = 0$.

The CLIC DR is a wiggler-dominated lattice, targeting ultra-low emittances in all three planes and small damping times. The output emittances are strongly dominated by the IBS effect; thus, it is an interesting testbed for the comparison between different theoretical models and the multi-particle tracking code SIRE, in the presence of synchrotron radiation and quantum excitation. Table 1 summarizes some basic lattice and beam properties of the CLIC DRs lattice design [20].

Table 1: Basic equilibrium lattice parameters for the CLIC DR lattice.

Parameter	***Value***
Energy [GeV]	2.86
Circumference [m]	427.5
Bunch population [10^{11}]	4.1
Hor. emittance [nm rad] w/wo IBS	0.056
Vert. emittance [pm rad] w/wo IBS	0.56
Bunch length [mm] w/wo IBS	1.6
Energy spread w/wo IBS	1e-3
Damping times [tau_x/tau_y/tau_l] [ms]	2/2/1

For the IBS growth rate calculations, the IBS kicks are distributed over an adequate amount of points across the ring, such that the variation of the optics is taken into account and the areas were IBS is predominant are well represented. Table 2 summarizes the steady state horizontal geometrical emittance as estimated by the theoretical models of Bjorken-Mtingwa (BM) and Piwinski (Piw.) and the high energy approximations of Bane [21] and CIMP [4]. BM, Bane and CIMP are in good agreement, while Piwinski underestimates the effect with respect to the other three. The same study was performed for other low emittance lattices as well, coming to the same conclusion: In regimes where the IBS effect acts as a perturbation, all theoretical models are in very good agreement while in regimes where the steady state emittances are dominated by the IBS effect, the theoretical models diverge [22].

Table 2: Steady state hor. emittance calculated by BM, P, Bane and CIMP for the CLIC DR.

Parameter (model)	ε_x ***(BM)***	ε_x ***(Piw.)***	ε_x ***(Bane)***	ε_x ***(CIMP)***
Steady state emittance [pm-rad]	95.4	85.8	98.1	97.2

Figure 5 shows a comparison between the theoretical models of Bjorken-Mtingwa and Piwinski with the multi-particle tracking code SIRE for one turn of the CLIC DR lattice. As SIRE is a Monte-Carlo code, the tracking simulations were performed several times and the

one standard deviation error-bars are also shown in the plots. The results from SIRE simulations are shown in green, from Bjorken-Mtingwa in black, from Piwinski in red and from Bane in magenta. The classical formalism of Piwinski is in perfect agreement with the SIRE results, in all planes. This is not a surprise, as both Piwinski formalism and the tracking codes use the Rutherford cross-section, to calculate the scattering probability in a solid angle. All theories and simulations predict the same trend for the emittance evolution along the ring and are in fairly good agreement within 3σ in all planes.

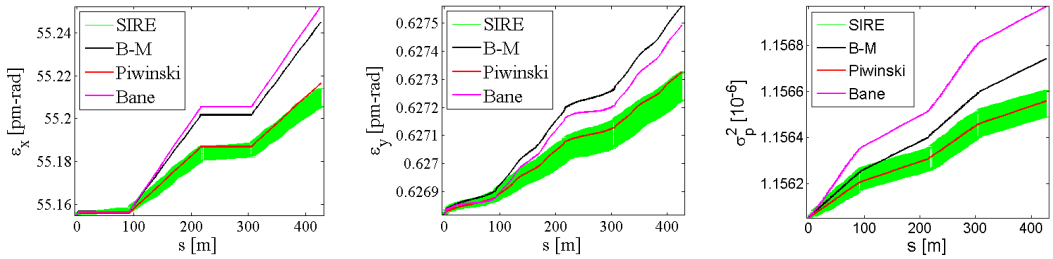

Figure 5: One turn comparison for the horizontal (left) and vertical (middle) emittance and energy spread (right) between the tracking code SIRE (green) and the theoretical models BM (black), Piwinski (red) and Bane (magenta) for the CLIC DR lattice.

For the LHC/HL-LHC proton beams at collision energy, synchrotron radiation turns into a perceptible effect as well. It continuously shrinks the emittances with damping times of 12.9 h in the longitudinal plane and of 26.0 h in the two transverse planes. The effects of IBS and SRD on the expected evolution of the LHC and SLHC beam emittances during physics coasts at 7 TeV were examined in [23] and SIRE was benchmarked against the Bjorken-Mtingwa formalism for different cases.

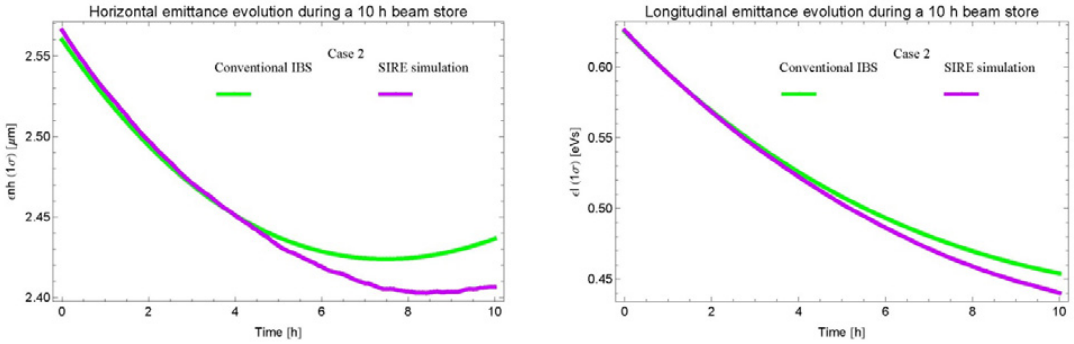

Figure 6: Comparison of ε_H^N (left) and ε_L (right) between SIRE (magenta) and analytical IBS (B-M) (green) computations (case 2, Table 1): difference $\delta_{max}(\Delta\varepsilon_H/\varepsilon_H) \sim 1\%$ and $\delta_{max}(\Delta\varepsilon_L/\varepsilon_L) \sim 2\%$.

Figure 6 compares the evolution of the emittances for the first IR upgrade with reduced emittances [23] between SIRE simulation and the straight IBS computation, taking into account the joint effects of IBS and radiation damping. Including quantum excitation effect in Bjorken-Mtingwa calculations would yield negligible change of the LHC proton beam equilibrium emittances (assuming 1% coupling between the horizontal and vertical planes). Examination of the joint intrabeam and synchrotron radiation damping phenomena during a 10 hours physics beam store at 7 TeV in the first IR upgrade of LHC shows that over the

full physics fill duration the evolution of emittances is kept inside the design values, as the IBS growth is largely balanced by the synchrotron radiation damping.

Even though SIRE simulation algorithm and Bjorken-Mtingwa analytical formalism make use of distinct approaches to tackle the IBS issue, both techniques agree rather well.

2.4.6 **Summary**

The conventional IBS Piwinski and Bjorken-Mtingwa formalisms for bunched beams and the Zenkevich Monte Carlo IBS simulation formalism based on binary collision models have been reviewed.

The Piwinski formalism is using the "classical" Rutherford differential cross-section for the Coulomb scattering. Unlike Piwinski, the approach to IBS of Bjorken and Mtingwa is based on the time-evolution operator « S-matrix » that relates transitions from an initial quantum state $|i\rangle$ to a final state $|f\rangle$ of a physical system experiencing a scattering process. Both models consider Gaussian laws for the beam density distributions in phase space in order to derive analytical formulas for the IBS rise times.

Other IBS models based on non-Gaussian distributions have been formulated using the kinetic analysis for the modelling of small angle multiple Coulomb scattering. Zenkevich's approach was to develop a Monte Carlo based macro-particle algorithm called "binary collision map" (BCM), realized in the macro-particle code "Monte-Carlo code" (MOCAC) for numerical modelling of IBS effects in accelerators and storage rings. An extension of it called "Software for Intrabeam Scattering and Radiation effects" (SIRE) was developed to simulate the evolution of beam particle distributions in storage rings, taking into account IBS, radiation damping and quantum excitation.

A benchmarking of the IBS theoretical models with the Monde Carlo SIRE code for the case of the CLIC Damping Rings, which is an intrabeam scattering dominated ring in the presence of strong synchrotron radiation and for the LHS/HL-LHC proton beams at collision energy, where synchrotron radiation turns into a noticeable effect as well, shows very good agreement of the simulation tools and the conventional models.

2.4.7 **Acknowledgements**

We warmly acknowledge the major contribution of P. Zenkevich to the ideas leading to the development of an IBS Monte-Carlo code and to A. Vivoli for the development of SIRE and many fruitful discussions. We would like also to thank C. Carli for his contribution in the production of the plot in Fig. 2.

2.4.8 **References**

1. A. Piwinski, "Intra-beam scattering", Proc. 9th Int. Conference on High Energy Accelerators, Stanford, CA, 1974 (SLAC, Stanford, CA, 1974), p. 405.
2. J. Bjorken, S. Mtingwa, "Intrabeam scattering", Part. Accel. 13 (1983) 115.
3. F. Antoniou, F. Zimmermann, "Revision of intrabeam scattering with non-ultrarelativistic corrections and vertical dispersion for MAD-X", CERN-ATS-2012-066 (2012).
4. K. Kubo, S. Mtingwa, A. Wolski, "Intrabeam scattering formulas for high energy beams" (2005) 081001. http://dx.doi.org/10.1103/PhysRevSTAB.8.081001.
5. A. Woslki, "Beam dynamics in high energy particle accelerators", Imperial College

Press, March 2014.
6. A. Woslki, "Space Charge, Intrabeam scattering and Touschek effects", Fourth International Accelerator School for Linear Colliders, Beijing, September 2009. http://uspas.fnal.gov/materials/12MSU/DampingRings-Lecture6.
7. L. Evans and B. Zotter, "Intrabeam scattering in the SPS", CERN/SPS/80-15-DI (1980).
8. M. Martini, “Intrabeam scattering in the ACOL-AA machines”, CERN PS/84 9 (1984).
9. M. Martini, “Intrabeam scattering: Anatomy of the theory”, Proc. CAS–CERN Accelerator School “Intensity Limitations in Particle Beams”, Geneva, November 2015.
10. J. Bjorken, S. Drell, “Relativistic quantum mechanics“, McGraw-Hill, New York, (1964).
11. P. Zenkevich, “Last advances in analysis of intra-beam scattering in the hadron storage rings”, Nuclear Instruments and Methods in Physics Research (2007), http://dx.doi.org/10.1016/j.nima.2007.02.04.
12. P. Zenkevich, A. Bolshakov, O. Boine-Frankenheim, “Kinetic effects in multiple intra-beam scattering”, ICFA HB204, Bensheim, 2005 [AIP Conf. Proc. 773 (2005) 425].
13. N. Alekseev, A. Bolshakov, E. Mustafin, P. Zenkevich, “Numerical code for Monte-Carlo simulation of ion storage”, [AIP Conf. Proc. 480 (1999) 31], http://scitation.aip.org/content/aip/proceeding/aipcp/480?ver=pdfcov.
14. M. Martini, A. Vivoli, “Effect of intrabeam scattering and synchrotron radiation damping when reducing transverse emittances to augment the LHC luminosity”, CERN-sLHC-PROJECT-Report-0032 (2010).
15. T Akizuka, H. Abe, “A binary collision model for plasma simulation with a particle code”, Journal of computational physics 25 (1977).
16. J. Bittencourt, “Fundamentals of plasma physics” (Springer, New York, 2004).
17. P. Bellan, “Fundamentals of plasma physics” (Cambridge University Press, 2012).